Journal of Computational Physics **180,** 736–750 (2002)
doi:10.1006/jcph.2002.7120

Divergence- and Curl-Preserving Prolongation and Restriction Formulas

G. Tóth and P. L. Roe

University of Michigan, Ann Arbor, Michigan
E-mail: gtoth@umich.edu, philroe@umich.edu

Received October 20, 2000; revised May 23, 2002

We present new second-order prolongation and restriction formulas which preserve the divergence and, in some cases, the curl of a discretized vector field. The formulas are suitable for adaptive and hierarchical mesh algorithms with a factor-of-2 linear resolution change. We examine both staggered and collocated discretizations for the vector field on two- and three-dimensional Cartesian grids. The new formulas can be used in combination with numerical schemes that require a divergence-free solution in some discrete sense, such as the constrained transport schemes of computational magnetohydrodynamics. We also obtain divergence-preserving interpolation functions which may be used for streamline or field line tracing.

Key Words: numerical approximation; magnetohydrodynamics.

1. INTRODUCTION

Adaptive and hierarchical grids provide some of the most efficient spatial discretizations for multiscale computational problems. It is of great interest to extend numerical schemes designed for a simple structured mesh to adaptive and hierarchical grids. The critical issues of such an extension are (a) the prolongation, which is the interpolation of the solution on a coarse mesh to the finer mesh; (b) the restriction, which provides the mapping from the fine mesh solution to the coarse mesh; and (c) generalization of the scheme for resolution changes, which occur at the interfaces between fine and coarse meshes.

The prolongation and restriction operations should conserve the properties of the solution which are critical for the scheme, and these properties should also be defined appropriately at resolution changes. Some properties, such as the conservation of some scalar quantity (e.g., mass or energy), are relatively easy to preserve for an adaptive grid. For vector fields, however, more complicated issues can arise, for example, if it is required that the scheme preserves in some sense differential quantities such as the divergence or curl. For example, in incompressible hydrodynamics the divergence of the velocity field must remain zero

0021-9991/02 $35.00

(in some appropriate discrete sense) and in magnetohydrodynamics (MHD) the same is true of the divergence of the magnetic field. In both cases, there are numerical methods that rely on satisfying these constraints exactly for all time. In incompressible flow the MAC method [8] and its successors are of this type, and in MHD the constrained transport (CT) method [7] and its variants. It is not often a constraint that the curl vanishes, and when it is, a potential formulation can be employed. However, in fluid dynamics, especially in three dimensions (3D), the vorticity (which is defined as the curl of the velocity field), is an important quantity that can only be generated through rather specific physical mechanisms, but once it exists it may be convected over large distances. Therefore it is desirable that vorticity be created only by the proper mechanisms and not by numerical errors. Control over vorticity can be exerted by strategies similar to those employed to control divergence [11].

To extend schemes of this "constrained evolution" type to adaptive and hierarchical grids, we present formulas ensuring that the prolongation of a discrete vector field onto a refined grid will generate values of the discrete divergence and curl bounded by the values on the coarse grid. In particular, if the coarse field is divergence- or curl-free, then the refined field will be also. In different areas of computational physics, there are traditions concerning the representations of vector fields. For incompressible fluid mechanics it is common to store the normal components of the velocity on the faces of control volumes. In MHD, the normal components of the magnetic field are often stored in the same way. When dealing with Maxwell's equations, one may adopt Yee's strategy [16] of placing the magnetic field components normal to the faces and the electric field parallel to the edges (or vice versa), but this is equivalent to representing both fields normal to the faces of two overlapping grids. Each of these strategies may be described as staggered. By contrast, some schemes call for all variables to be stored in the same place, that is, to be collocated. This is important for Godunov-type schemes that use information derived from estimated wave strengths. Recently, there has been a trend to combine the two strategies by appropriately interpolating between the two differently stored fields [2, 4, 6, 9, 13, 15]. With respect to mesh refinement, collocation can be vertex based and cell-center based as shown in Fig. 1. We give results for two cases: staggered and vertex-based collocated storage. Cell-centered collocated storage does not seem to lend itself to divergence-preserving prolongation and

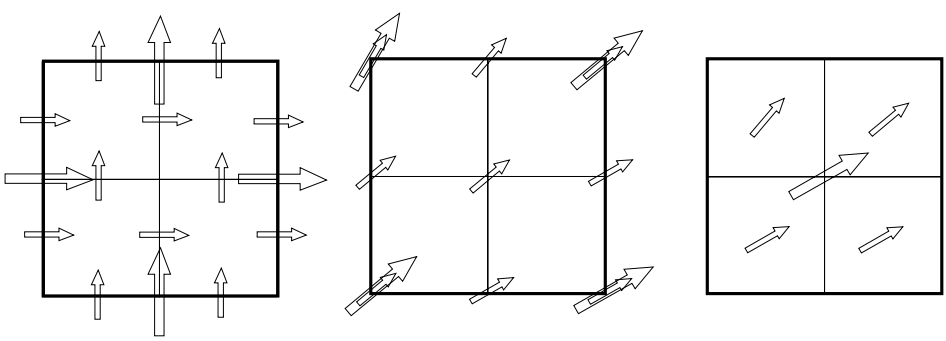

FIG. 1. Three possibilities for the storage of a 2D vector field showing the relative placement of coarse-(large arrows) and fine-resolution (small arrows) discretizations. The coarse cell (thick lines) is divided into four fine cells (thin lines).

restriction formulas, because the divergence or curl for a cell depends on the data in the possibly finer or coarser neighboring cell centers.

We present formulas for 3D Cartesian grids with resolution changes of a factor of 2. The simpler 2D case is also described. For structured, but non-Cartesian grids or for resolution changes that differ by more than a factor of 2, similar formulas can be derived following the ideas described in the following.

2. NOTATION

The vector field components parallel to the x, y, and z axes are denoted by $\tilde{U}$, $\tilde{V}$, and $\tilde{W}$ on the coarse grid, and by $\tilde{u}$, $\tilde{v}$, and $\tilde{w}$ on the fine grid, respectively. Although this notation is more common for the velocity field, for MHD cases they represent the magnetic field components. The coarse- and fine-grid cell spacings are ΔX, ΔY, ΔZ and $\Delta x = \Delta X/2$, $\Delta y = \Delta Y/2$, $\Delta z = \Delta Z/2$, respectively. When the aspect ratio of the computational cell is not unity, it greatly simplifies the derivations as well as the implementation, if fluxes are used instead of field components. Therefore we introduce the coarse fluxes $U = \Delta Y \Delta Z \tilde{U}$, $V = \Delta Z \Delta X \tilde{V}$, and $W = \Delta X \Delta Y \tilde{W}$ and the analogously defined fine fluxes u, v, and w. The volumes of the coarse and fine cells are $\Omega = \Delta X \Delta Y \Delta Z$ and $\omega = \Delta x \Delta y \Delta z = \Omega/8$, respectively.

3. FACE-CENTER-BASED FORMULATION

A finite volume adaptive grid consists of coarse and fine *cells*. When a coarse cell with its center at $x = y = z = 0$ is refined into eight smaller cells, the fine cell centers will be at $\pm\Delta x/2$, $\pm\Delta y/2$, $\pm\Delta z/2$ (see Fig. 2). Note that the fine cell centers are not coplanar with

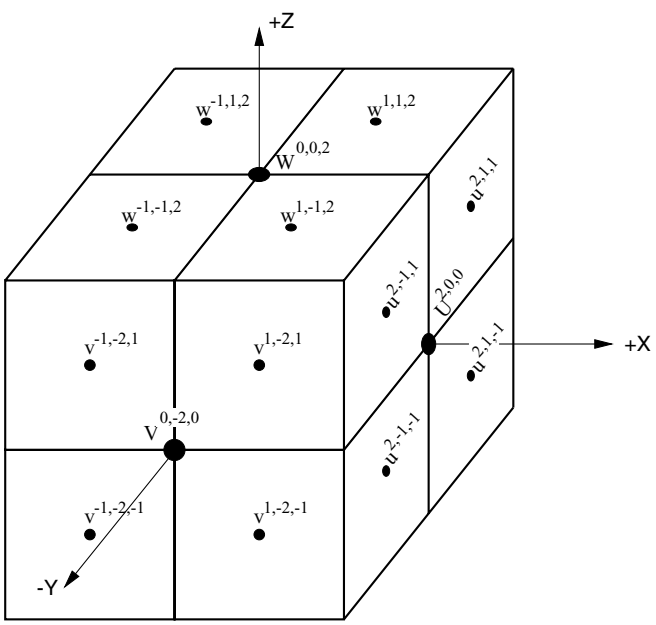

FIG. 2. The placement and notation of vector components for the face-centered discretization.

the coarse cell centers; on the other hand, the appropriate cell interfaces are coplanar. This simple observation implies that the divergence and curl of a vector field should be defined by the solution at cell interfaces, so that resolution changes can be handled consistently. The most natural choice for the definition of the divergence operator uses a staggered representation of the vector field, with the x, y, and z components defined at the cell face centers orthogonal to the x, y, and z directions, respectively [16]. To simplify the notation and to avoid fractional indices, the coarse cell center is at $i = j = k = 0$ and the six coarse cell faces are at $i = \pm 2$, $j = \pm 2$, and $k = \pm 2$, respectively. For the case $\Delta X = \Delta Y = \Delta Z = 4$ the i, j, k indices coincide with the x, y, z coordinates. The indices are written as superscripts, since subscripts will be used for other purposes. The 6 coarse vector field components are then $U^{\pm 2,0,0}$, $V^{0,\pm 2,0}$, and $W^{0,0,\pm 2}$, while the 36 fine vector field components are denoted by $u^{n,\pm 1,\pm 1}$, $v^{\pm 1,n,\pm 1}$, and $w^{\pm 1,\pm 1,n}$ with $n = -2, 0, 2$.

The coarse cell divergence of the vector field is defined as

$$\mathrm{D} = \frac{1}{\Omega}(U^{2,0,0} - U^{-2,0,0} + V^{0,2,0} - V^{0,-2,0} + W^{0,0,2} - W^{0,0,-2}) \tag{1}$$

while the eight fine cell divergences for i, j, $k = \pm 1$ are

$$\mathrm{d}^{i,j,k} = \frac{1}{\omega}(u^{i+1,j,k} - u^{i-1,j,k} + v^{i,j+1,k} - v^{i,j-1,k} + w^{i,j,k+1} - w^{i,j,k-1}). \tag{2}$$

3.1. Restriction Operator

For the restriction operator we require that $\Omega \mathrm{D} = \sum \omega \mathrm{d}^{i,j,k}$, which is quite easy to satisfy if the fluxes at the six interfaces are conserved; thus the restriction operator is uniquely given by

$$U^{\pm 2,0,0} = \sum_{j,k=\pm 1} u^{\pm 2,j,k}, \tag{3}$$

with similar equations for the V and W components. This is clearly a second-order restriction formula in the finite difference sense, since the difference between the interpolated $\tilde{U}$ and the "exact" value of the fine vector field $\tilde{u}$ obtained at the center of the coarse face from a Taylor series expansion is of the order of $(\Delta y)^2$, $(\Delta z)^2$, and $\Delta y \Delta z$.

3.2. Prolongation Operator

The prolonged solution should satisfy a flux conservation similar to (3), which means that the fine solution in the four quadrants can be written as

$$\begin{aligned} u^{\pm 2,j,k} &= \frac{1}{4}\left(U^{\pm 2,0,0} + jU_y^{\pm 2,0,0} + kU_z^{\pm 2,0,0}\right), \\ v^{i,\pm 2,k} &= \frac{1}{4}\left(V^{\pm 2,0,0} + kV_z^{0,\pm 2,0} + iV_x^{0,\pm 2,0}\right), \\ w^{i,j,\pm 2} &= \frac{1}{4}\left(W^{0,0,\pm 2} + iW_x^{0,0,\pm 2} + jW_y^{0,0,\pm 2}\right), \end{aligned} \tag{4}$$

for i, j, $k = \pm 1$. Here U_y, U_z, etc. are numerical approximations to the tangential slopes, or in physical terms the shear, based on the coarse solution. A simple central difference

formula for U_y would be

$$U_y^{2,0,0} = \frac{1}{8}(U^{2,4,0} - U^{2,-4,0}). \tag{5}$$

For certain applications and schemes, e.g., for total-variation-diminishing schemes, the slopes should be limited by an appropriate limiter.

If some of the faces of the coarse cell are shared with finer neighbor cells, then we should simply copy the fine fluxes from the neighboring cells instead of applying the formulas (4). The following results do not depend on how the prolonged solution is obtained on the surface of the coarse cell as long as the flux conservation is ensured.

To fully define the prolongation, we still need to determine the 12 vector components $u^{0,\pm1,\pm1}$, $v^{\pm1,0,\pm1}$, and $w^{\pm1,\pm1,0}$ which lie on the central fine cell interfaces. We require that the divergences defined in (1) and (2) satisfy

$$\mathrm{d}_{i,j,k} = \mathrm{D}, \tag{6}$$

for all $i = \pm1$, $j = \pm1$, $k = \pm1$. This gives seven independent equations for the 12 unknowns, so we still have five degrees of freedom. To make the interpolation formulas as symmetric and accurate as possible, we require that the six curls of the fine solution around the six fine cell edges starting from the origin have the same value as the curl estimated from the coarse cell solution. There is very little restriction on how the curl of the coarse solution should be evaluated, but it seems natural to use the average of the same partial derivatives as in (4). This leads to

$$\begin{aligned}
\sum_{t=\pm1} t[(\Delta z)^2 w^{\pm1,t,0} - (\Delta y)^2 v^{\pm1,0,t}] &= \frac{1}{2}\sum_{n,t=\pm1} t[(\Delta z)^2 w^{\pm1,t,2n} - (\Delta y)^2 v^{\pm1,2n,t}],\\
\sum_{t=\pm1} t[(\Delta x)^2 u^{0,\pm1,t} - (\Delta z)^2 w^{t,\pm1,0}] &= \frac{1}{2}\sum_{n,t=\pm1} t[(\Delta x)^2 u^{2n,\pm1,t} - (\Delta z)^2 w^{t,\pm1,2n}],\\
\sum_{t=\pm1} t[(\Delta y)^2 v^{t,0,\pm1} - (\Delta x)^2 u^{0,t,\pm1}] &= \frac{1}{2}\sum_{n,t=\pm1} t[(\Delta y)^2 v^{t,2n,\pm1} - (\Delta x)^2 u^{2n,t,\pm1}],
\end{aligned} \tag{7}$$

where only the left-hand sides contain unknowns. The $(\Delta x)^2$, $(\Delta y)^2$, and $(\Delta z)^2$ coefficients appear because we defined u, v, and w to be fluxes. Only five of these equations are independent, which can be checked by adding them up with alternating signs. With the aid of MAPLE Eqs. (6) and (7) can be solved, and after some simplification the prolongation formulas

$$u^{0,j,k} = \frac{1}{2}(u^{2,j,k} + u^{-2,j,k}) + U_{xx} + k(\Delta z)^2 V_{xyz} + j(\Delta y)^2 W_{xyz}, \tag{8}$$

$$v^{i,0,k} = \frac{1}{2}(v^{i,2,k} + v^{i,-2,k}) + V_{yy} + i(\Delta x)^2 W_{xyz} + k(\Delta z)^2 U_{xyz}, \tag{9}$$

$$w^{i,j,0} = \frac{1}{2}(w^{i,j,2} + w^{i,j,-2}) + W_{zz} + j(\Delta y)^2 U_{xyz} + i(\Delta x)^2 V_{xyz}, \tag{10}$$

for $i, j, k = \pm1$, are obtained. The second- and third-order derivatives are defined as

$$U_{xx} = \frac{1}{8}\sum_{i,j,k=\pm1} ijv^{i,2j,k} + ikw^{i,j,2k} \propto \frac{\partial^2 V}{\partial y \partial x} + \frac{\partial^2 W}{\partial z \partial x}, \tag{11}$$

$$U_{xyz} = \frac{1}{8}\sum_{i,j,k=\pm 1} \frac{ijku^{2i,j,k}}{(\Delta y)^2 + (\Delta z)^2} \propto \frac{\partial^3 U}{\partial x \partial y \partial z}. \tag{12}$$

When the divergence of the vector field is constant in space, in particular, if it is 0 everywhere, $U_{xx} \propto \partial^2 U/(\partial x)^2$. The prolongation formulas (4) and (8)–(10) are clearly second-order accurate. We note that the third-order terms U_{xyz}, V_{xyz}, and W_{xyz} disappear on faces of the coarse cell where the prolonged solution is determined with (limited) linear interpolation (4), but it is nonzero if the prolonged solution is copied from neighboring finer cells.

In the 2D case there are three independent divergence constraints and just one curl constraint for the inner four fine vector components $u^{0,\pm 1}$, $v^{\pm 1,0}$. The results have the same form as (8) and (9); however, in 2D all the third-order derivatives in (12) are identically zero, while the second-order derivatives simplify to $U_{xx} = (v^{-1,-2} - v^{-1,2} - v^{1,-2} + v^{1,2})/4$ and $V_{yy} = (u^{-2,-1} - u^{2,-1} - u^{-2,1} + u^{2,1})/4$.

3.3. Continuous Interpolation

The prolongation formulas in the previous section define the refined vector field in a finite set of points, ensuring that the discrete divergence and curl are preserved. One may continue to refine the cells to find more and more points until we arrive at a continuous function which has the same divergence and curl as the original discrete vector field. Alternatively, we can try to find simple interpolating polynomials based on the discrete formulas and verify that they have the desired properties. Divergence-free interpolation can be useful for tracing magnetic field lines or streamlines of an incompressible fluid based on the discrete solution.

In 2D, let us scale the coordinates so that the computational cell occupies the $-1 < x, y < 1$ square. The discrete face-center values are $U(\pm 1, 0)$ and $V(0, \pm 1)$ and we also have some numerical approximations of the transverse gradients $U_y(\pm 1, 0)$ and $V_x(0, \pm 1)$. To make the notation more compact, we use upper indices instead of coordinates. Given these point values, we define the continuous interpolation functions as

$$\begin{aligned} U(x, y) &= \frac{1+x}{2}\left(U^{1,0} + yU_y^{1,0}\right) + \frac{1-x}{2}\left(U^{-1,0} + yU_y^{-1,0}\right) + \frac{1-x^2}{4}\left(V_x^{0,1} - V_x^{0,-1}\right), \\ V(x, y) &= \frac{1+y}{2}\left(V^{0,1} + xV_x^{0,1}\right) + \frac{1-y}{2}\left(V^{0,-1} + xV_x^{0,-1}\right) + \frac{1-y^2}{4}\left(U_y^{1,0} - U_y^{-1,0}\right). \end{aligned} \tag{13}$$

The first two terms on the right-hand sides are generalizations of (4), while the third terms correspond to U_{xx} and V_{yy} in (8) and (9). It is easy to show that the divergence

$$\frac{\partial U}{\partial x} + \frac{\partial V}{\partial y} = \frac{U^{1,0} - U^{-1,0}}{2} + \frac{V^{0,1} - V^{0,-1}}{2} \tag{14}$$

everywhere within the cell. The z component of the curl is

$$\frac{\partial V}{\partial x} - \frac{\partial U}{\partial y} = \frac{(1+y)V_x^{0,1} + (1-y)V_x^{0,-1}}{2} - \frac{(1+x)U_x^{1,0} - (1-x)U_x^{-1,0}}{2}, \tag{15}$$

which is not a constant; rather, it is a linear interpolation of the discrete derivatives that define the discrete curl and thus should be well behaved.

The interpolation functions (13) are continuous across cell boundaries in the normal component, but they are discontinuous in the transverse component in general because the transverse gradients U_y and V_x cannot make a perfect match at both sides of the cell. The discontinuity vanishes with increasing grid resolution at a second-order rate. Given the constraints on flux conservation, the discontinuity is unavoidable for these low-order polynomials.

The 3D generalization of the 2D interpolation polynomials is straightforward:

$$U(x, y, z) = \frac{1+x}{2}\left(U^{1,0,0} + yU_y^{1,0,0} + zU_z^{1,0,0}\right) + \frac{1-x}{2}\left(U^{-1,0,0} + yU_y^{-1,0,0} + zU_z^{-1,0,0}\right) + \frac{1-x^2}{4}\left(V_x^{0,1,0} - V_x^{0,-1,0} + W_x^{0,0,1} - W_x^{0,0,-1}\right). \quad (16)$$

$V(x, y, z)$ and $W(x, y, z)$ are defined analogously. The divergence of the interpolated vector field is constant and equal to the discrete divergence. The curl also behaves the same way as in the 2D case. Note that the third-order terms, like V_{xyz} or W_{xyz} in (8), do not occur in the continuous interpolation functions.

4. VERTEX-BASED FORMULATION

In a vertex-based discretization all components of the vector field are collocated at the vertices. The coarse-grid vertices are at $\pm\Delta X/2, \pm\Delta Y/2, \pm\Delta Z/2$ indexed by $i, j, k = \pm 2$, while the fine-grid vertices are at $(0, \pm\Delta x)$, $(0, \pm\Delta y)$, $(0, \pm\Delta z)$ indexed by $i, j, k = -2$, 0, 2. Here the coarse vertices coincide with a subset of the fine vertices, unlike in a cell-centered adaptive grid (see the middle panel of Fig. 1).

4.1. Prolongation Operator

For the coinciding vertices it is natural to make the coarse and fine solutions equal; i.e.,

$$\tilde{u}^{\pm 2,\pm 2,\pm 2} = \tilde{U}^{\pm 2,\pm 2,\pm 2}. \quad (17)$$

We note, however, that this natural choice only works for the prolongation operator. For a divergence-free restriction operator one needs to use a more general prescription. We will return to the restriction operator in Section 4.2.

Edges and faces are shared by four and two cells respectively. Consequently, they should be prolonged with the use of data residing on the given edge or face otherwise the prolonged solution could become multivalued for the same location. For edge centers this gives the following second-order interpolations:

$$\begin{aligned} u^{0,\pm 2,\pm 2} &= \frac{1}{2}(u^{-2,\pm 2,\pm 2} + u^{2,\pm 2,\pm 2}), \\ u^{\pm 2,0,\pm 2} &= \frac{1}{2}(u^{\pm 2,-2,\pm 2} + u^{\pm 2,2,\pm 2}), \\ u^{\pm 2,\pm 2,0} &= \frac{1}{2}(u^{\pm 2,\pm 2,-2} + u^{\pm 2,\pm 2,2}). \end{aligned} \quad (18)$$

The edge-centered v and w components are obtained analogously. We also require that the flux through one face of the coarse cube is unchanged by the prolongation. The flux is

defined as the average of the normal component at the four vertices of the face; for example, the coarse and fine fluxes in the x direction are

$$F^{i,0,0} = \frac{1}{4} \sum_{l,m=\pm 2} U^{i,l,m}, \qquad i = \pm 2, \tag{19}$$

$$f^{i,j,k} = \frac{1}{4} \sum_{l,m=\pm 1} u^{i,l+j,k+j}, \quad i = -2, 0, 2 \quad j,k = \pm 1, \tag{20}$$

and we require that the fine fluxes add up to the coarse flux,

$$\sum_{j,k=\pm 1} f^{\pm 2,j,k} = F^{\pm 2,0,0}. \tag{21}$$

The g, h and G, H fluxes in the y and z directions and the corresponding flux conservation equations are defined similarly. From the corner and edge interpolation formulas (17) and (18) it follows that the orthogonal component at the face center must be a simple average of the corner values,

$$u^{\pm 2,0,0} = \frac{1}{4} \sum_{j,k=\pm 2} u^{\pm 2,j,k}, \tag{22}$$

and similar equations apply to $v^{0,\pm 2,0}$ and $w^{0,0,\pm 2}$. The flux conservation will also ensure that the average of the eight fine divergences equals the divergence over the coarse cell.

There are still 15 unknowns to determine: the 12 tangential components at the center of the coarse faces and the 3 components at the central fine vertex. The prolongation is constrained by the requirement that the divergences in the fine cells are all equal to each other and thus to one-eighth of the coarse divergence. For the vertex-based formulation we define the divergences in terms of the face-centered fluxes as

$$\mathrm{D} = \frac{1}{\Omega}(F^{2,0,0} - F^{-2,0,0} + G^{0,2,0} - G^{0,-2,0} + H^{0,0,2} - H^{0,0,-2}), \tag{23}$$

$$\mathrm{d}^{i,j,k} = \frac{1}{\omega}(f^{i+1,j,k} - f^{i-1,j,k} + g^{i,j+1,k} - g^{i,j-1,k} + h^{i,j,k+1} - h^{i,j,k-1}), \tag{24}$$

for $i, j, k = \pm 1$. Note that this definition is different from the simplest central difference formula in terms of the vector field components, since we average in the tangential directions in (19) and (20). The advantage of this definition is that the coarse cell divergence is the average of the fine cell divergences.

Besides the restriction (6) that the fine divergences are all equal, there is another constraint to be met: Interpolation to the center of a face should only involve data on that face, so that adjacent large cubes should be compatible. With the requirements of second-order accuracy and rotational and mirror symmetry, the three vector components at the four corners of the face can only be combined as

$$u^{0,\pm 2,0} = \frac{1}{4} \sum_{i,k=\pm 2} u^{i,\pm 2,k} + ik(\alpha u^{i,\pm 2,k} + \beta v^{i,\pm 2,k} + \gamma w^{i,\pm 2,k}), \tag{25}$$

$$u^{0,0,\pm 2} = \frac{1}{4} \sum_{i,j=\pm 2} u^{i,j,\pm 2} + ij(\alpha u^{i,j,\pm 2} + \gamma v^{i,j,\pm 2} + \beta w^{i,j,\pm 2}), \tag{26}$$

where α, β, and γ are free parameters. The corresponding formulas for v and w can be obtained from cyclic permutations.

With the aid of MAPLE the eight divergence equations can be solved for the unknowns α, β, γ, $u^{0,0,0}$, $v^{0,0,0}$, and $w^{0,0,0}$. Although there are seven independent equations and only six unknowns, due to the good choice of parameters, we can find a whole family of solutions parameterized by α: $\beta = -\alpha$, $\gamma = 1/8$, and the vector components for the central vertex are some linear combinations of the coarse solution and α. The simplest and most natural choice is $\alpha = \beta = 0$, which gives

$$u^{0,\pm 2,0} = \frac{1}{4} \sum_{i,k=\pm 2} u^{i,\pm 2,k} + \frac{ik}{8} w^{i,\pm 2,k}, \tag{27}$$

$$u^{0,0,\pm 2} = \frac{1}{4} \sum_{i,j=\pm 2} u^{i,j,\pm 2} + \frac{ij}{8} v^{i,j,\pm 2}, \tag{28}$$

$$u^{0,0,0} = \frac{1}{8} \sum_{i,j,k=\pm 2} u^{i,j,k} + \frac{3ij}{8} v^{i,j,k} + \frac{3ik}{8} w^{i,j,k}, \tag{29}$$

and the prolongation formulas for v and w can be obtained with cyclic permutations. The prolongation formulas (18), (22), and (27)–(29) are all second-order accurate.

There is a simple reduction to the 2D case. The fine vector field at the edge centers of the coarse cell are defined as linear interpolations of the corresponding corner values, while the solution at the center of the coarse cell will be

$$u^{0,0} = \frac{1}{4} \sum_{i,j=\pm 2} u^{i,j} + \frac{3ij}{8} v^{i,j}, \tag{30}$$

$$v^{0,0} = \frac{1}{4} \sum_{i,j=\pm 2} v^{i,j} + \frac{3ij}{8} u^{i,j}. \tag{31}$$

4.2. Restriction Operator

It does not seem to be possible to design a local divergence-preserving restriction operator for the vertex-based storage. To see this, suppose that we want to coarsen eight fine cells into a single coarse cell while leaving all the neighboring fine cells unchanged. All the vector components collocated at the eight corners of the coarse cell are shared with neighboring fine cells; actually each coarse vertex is shared with seven fine cells. Therefore it is quite difficult to change the solution at the corners without changing the divergences in the fine cells sharing the same corner. On the other hand, if we keep the fine solution unchanged in the corner vertices of the coarse cell, the coarse divergence (23) will not be the average of the eight fine divergences (24) in general. This is because the fine vector components at the edge and face centers of the coarse cell contribute to $\sum_{i,j,k=\pm 1} \mathrm{d}^{i,j,k}$, as can be seen from substituting (20) into (24).

It is still possible to design a *global* divergence-preserving restriction operator, which should be applied to all cells in the computational domain. Multigrid applications, for example, require such global restriction operators. The basic idea is that the coarse solution must contain the sum of fine fluxes from the surrounding fine cells. When the coarse values are combined into coarse fluxes (19) and added to obtain a coarse divergence (23), the result

should be identical to the sum of fine fluxes over a closed surface. This goal is achieved by the second-order restriction formulas

$$U^{i,j,k} = \frac{1}{2} \sum_{l=\pm 2\ m,n=\pm 1} f^{i+l,j+m,k+n},$$
$$V^{i,j,k} = \frac{1}{2} \sum_{m=\pm 2\ l,n=\pm 1} g^{i+l,j+m,k+n}, \tag{32}$$
$$W^{i,j,k} = \frac{1}{2} \sum_{n=\pm 2\ l,m=\pm 1} h^{i+l,j+m,k+n},$$

where f, g, and h are defined in (20). With these second-order restriction formulas, the coarse divergence will be the average of the fine divergences in the 64 fine cells touching the coarse cell from inside and outside.

5. PROJECTION

In the previous sections we presented restriction and prolongation operators that use local information only, and they preserve the divergence (and in some cases the curl) of the vector field because of the carefully chosen difference formulas. A more general, but also more costly, approach to the problem is the use of operators with global dependence on the data.

One can obtain a divergence-free prolongation or restriction algorithm by using some arbitrary interpolation formulas to obtain an intermediate restricted or prolonged solution u^*, v^*, w^*, and then by projecting the intermediate solution to a divergence-free solution. The same idea, but in a different context, has been described earlier (e.g., [3]). For sake of completeness we present the algorithm here in our notation. The projection consists of two steps: First, we solve an appropriate discretization of the Poisson equation

$$\nabla^2 \phi = \frac{\partial u^*}{\partial x} + \frac{\partial v^*}{\partial y} + \frac{\partial w^*}{\partial z} \tag{33}$$

for the scalar field ϕ, and then we correct the field components as

$$u = u^* - \frac{\partial \phi}{\partial x},$$
$$v = v^* - \frac{\partial \phi}{\partial y}, \tag{34}$$
$$w = w^* - \frac{\partial \phi}{\partial z}.$$

It was shown by Tóth [15] that even for discontinuous vector fields, the projection step gives a consistent solution with the same order of accuracy as the order of the preliminary solution as long as (i) the Poisson and the correction equations are discretized and solved to the same or higher order of accuracy and (ii) a divergence-free solution of this order of accuracy exists. The discrete Laplace operator in the Poisson equation (33) must be the combination of the discrete gradient operator applied in the correction equation (34) with the discrete divergence operator applied on the preliminary solution in (33), so that the projected solution will be divergence-free in the discrete sense.

6. NUMERICAL EXAMPLE

We show results for the face-centered formulation defined by Eqs. (4) and (8)–(10). For (4) minmod limited slopes are used when there are no neighboring finer cells. These restriction and prolongation formulas have been implemented in the parallel 3D MHD code BATSRUS, which uses block adaptive mesh refinement [12]. In MHD, the three vector components U, V, and W correspond to the three components of the magnetic field B_x, B_y, and B_z, respectively. In these tests the magnetic field is evolved with the flux-averaged constrained transport scheme [2, 15] generalized for the block adaptive mesh refinement (AMR) grid. The generalization is quite straightforward. The only nontrivial part is the correction of the electric field at resolution changes: The electric field defined on coarse edges should be replaced with the average of the electric fields of the finer grid sharing the same edge. The constrained transport scheme is combined with a dimensionally unsplit second-order Godunov-type scheme (artificial wind [14]) using limited reconstrucion for the cell interfaces. The combined scheme is fully conservative, second order in space and time, and conserves the divergence of the magnetic field.

The test problem is the Kelvin–Helmholtz instability in the presence of a magnetic field. The same problem has been discussed in [10], where the problem was solved on a static grid in 2D. For sake of completeness the test problem is described here too. The ideal MHD equations are solved with inifinite conductivity. The initial condition has uniform density $\rho = 1$, pressure $p = 1$, and magnetic field $B_y = 0.129$, $B_x = B_z = 0$. The magnetic field is in normalized units in which the Alfvén speed is simply $v_A = |B|/\sqrt{\rho} = 0.129$. The adiabatic index is $\gamma = 5/3$ so that the sound speed is $c_s = \sqrt{\gamma p/\rho} = 1.29 = 10 v_A$. The shear flow is given by $u_y = 0.645 \tanh(x/0.05)$, which has a smooth transition of width 0.05 at the $x = 0$ plane. The amplitude of the shear flow corresponds to Mach number 0.5 and Alfvénic Mach number 5. There is no flow in the z direction; i.e., $u_z = 0$. The instability is initiated with a small velocity perturbation within $|x| < 0.2$ of the form $u_x = 0.01 \exp(-(x/0.2)^2) \cos(2\pi y)$. Outside the $|x| < 0.2$ strip $u_x = 0$.

The perturbation has a wavelength of 1 in the y direction, so the simulation domain is taken to be $|x| < 1$, $|y| < 0.5$, and $|z| < 0.5$ with periodic boundaries at $y = \pm 0.5$ and

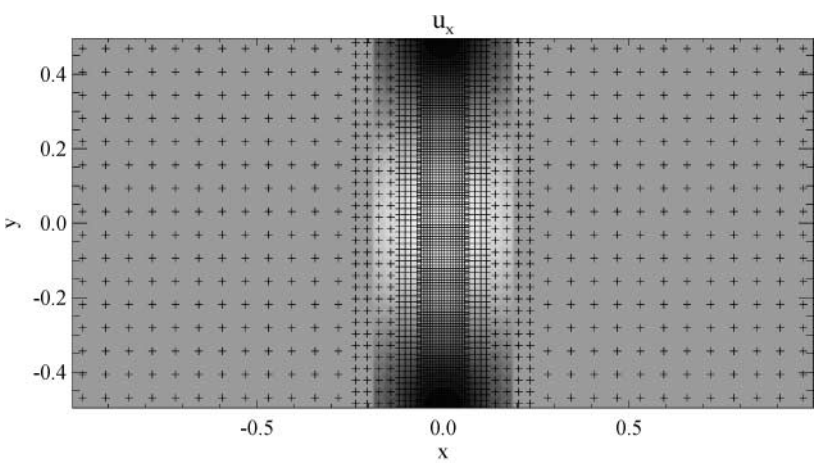

FIG. 3. The initial grid. Cell centers are shown as + signs. The velocity perturbation u_x is plot in gray scale in the range -0.01 (white) to 0.01 (black).

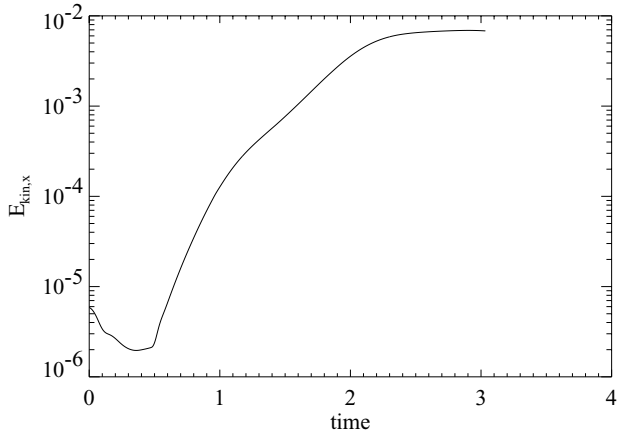

FIG. 4. The growth of the initial perturbation. The integrated kinetic energy in the x direction, $\rho u_x^2/2$, is plotted against time.

$z = \pm 0.5$. The size of the box in the x direction is sufficiently large so that the zero-gradient boundary conditions at $x = \pm 1$ do not influence the results during the simulation.

The initial grid is shown in Fig. 3. The grid is built up from 4832 blocks, each consisting of $4 \times 4 \times 4$ cells. The cell sizes vary between $1/16$ and $1/128$, and the finer cells are concentrated along the $x = 0$ plane. The grid is coarsened and refined every 300 time steps. The criterion for refinement is the vorticity $\nabla \times \mathbf{u}$, and about 20% of the cells are refined and coarsened each time. The total number of blocks is limited to 5000, which corresponds

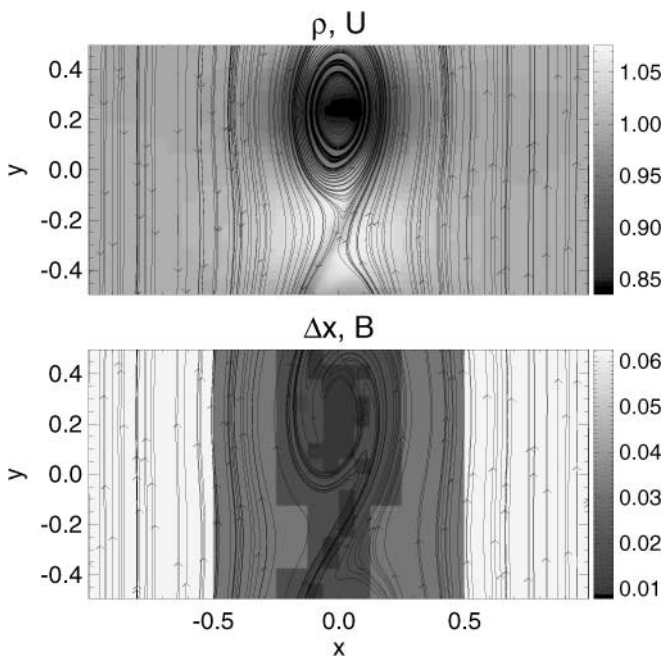

FIG. 5. The solution and the grid at time $t = 3.033$. Streamlines and density (top) and magnetic field lines and grid resolution (bottom) are shown.

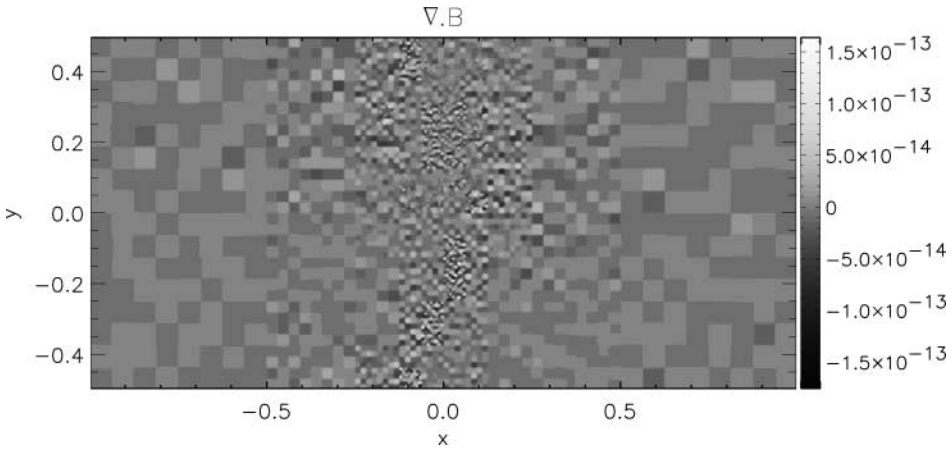

FIG. 6. The divergence of the magnetic field at time $t = 3.033$.

to 320,000 cells. Since the total number of refined and coarsened cells is limited irrespective of the symmetries of the solution, the initial translational invariance in the z direction is lost during the simulation. Once the resolution varies in the z direction, so will the solution, which is Kelvin–Helmholtz unstable.

The simulation is run for 2000 time steps, which corresponds to $t = 3.033$. By this time the instability has become nonlinear and has already saturated. The time dependence of the average kinetic energy in the x direction, $\rho u_x^2/2$, is shown in Fig. 4. The solution and the grid at this time are shown in Fig. 5. Although the grid went through six adaptation by this time, the divergence of the magnetic field remains zero to machine precision, as shown in Fig. 6, which demonstrates the correctness of the restriction and prolongation formulas as well as of the implementation.

We note that BATSRUS contains several other means of controlling the error in the divergence of the magnetic field, such as the 8-wave scheme [12], the diffusive control or parabolic approach [5], and the projection scheme [3]. The quantitative evaluation and comparison with these alternative approximations, however, would take us beyond the scope of this paper. Many of these schemes were compared on uniform grids in [15].

The initial condition of this test problem has a uniform magnetic field, which is divergence-free in the numerical sense (1) automatically. For less fortunate cases, the projection of the initial condition to a divergence-free face-centered magnetic field (33), (34) has also been implemented in BATSRUS, and it works as expected.

7. CONCLUSION

We designed restriction and prolongation operators that work for face-centered staggered and vertex-centered collocated vector fields in two and three dimensions. For the face-centered storage both the prolongation and restriction operators can act locally; thus they can be used for adaptive, hierarchical, and multigrid type schemes. For the vertex-based storage the prolongation operator is general, but the restriction operator only works if it is applied globally. Therefore the vertex-based restriction operator can be used for multigrid schemes, but not in the adaptive mesh refinement context. This suggests the use of face-centered storage for AMR schemes which require the divergence-free property.

It appears that for cell-centered collocated storage divergence-preserving restriction and prolongation operators can only be defined in a global sense, e.g., for multigrid, but we did not explore these possibilities. On the other hand, we showed how global divergence cleaning can be used to obtain high-order divergence-free solutions. If restriction and prolongation are not applied too frequently, e.g., for AMR, projection is a very general solution to the problem. Projection can also be used to obtain a numerically divergence free initial condition from an analytic solution or from a solution obtained with a non-divergence-free scheme.

Finally, the prolongation formulas derived for the staggered discretization were generalized to divergence-preserving interpolation functions. These interpolation functions can be used for tracing streamlines and field lines based on a discrete solution. If the discrete solution is divergence-free and the tracing algorithm is sufficiently accurate, the use of the divergence-preserving functions guarantees that there are no sources or sinks of the vector field even at a finite resolution, so the traced streamlines or field lines have the correct connectivity.

We demonstrated that the face-center-based formulation works in practice for adaptive mesh refinement. The quantitative evaluation and comparison with alternative approximations, however, would take us beyond the scope of this paper.

ACKNOWLEDGMENTS

G.T. has been partly supported by the Education Ministry of Hungary (Grant FKFP-0242-2000) and the Hungarian Science Foundation (OTKA, Grant T037548). During the review process of this paper Balsara submitted and published a paper [1] which contains formulas for the face-center-based formulation similar to those derived here. The results in his and our papers were obtained independently and in a different manner. The only changes made in this paper based on Balsara's results are the remarks concerning the case where the prolonged cell shares one or more faces with already finer cells, but none of our formulas required any changes.

REFERENCES

1. D. S. Balsara, Divergence-free adaptive mesh refinement for magnetohydrodynamics, *J. Comput. Phys.* **174**, 614 (2001), doi:10.1006/jcph.2001.6917.
2. D. S. Balsara and D. S. Spicer, A staggered mesh algorithm using high order Godunov fluxes to ensure solenoidal magnetic fields in magnetohydrodynamic simulations, *J. Comput. Phys.* **149**, 270 (1999), doi:10.1006/jcph.1998.6153.
3. J. U. Brackbill and D. C. Barnes, The effect of nonzero $\nabla \cdot \mathbf{B}$ on the numerical solution of the magnetohydrodynamic equations, *J. Comput. Phys.* **35**, 426 (1980).
4. W. Dai and P. R. Woodward, A simple finite difference scheme for multidimensional magnetohydrodynamic equations, *J. Comput. Phys.* **142**, 331 (1998), doi:10.1006/jcph.1998.5944.
5. A. Dedner, F. Kemm, D. Kröner, C.-D. Munz, T. Schnitzer, and M. Wesenberg, Hyperbolic divergence cleaning for the MHD equations, *J. Comput. Phys.* **175**, 645 (2002), doi:10.1006/jcph.2001.6961.
6. C. R. DeVore, Flux-corrected transport techniques for multidimensional compressible magnetohydrodynamics, *J. Comput. Phys.* **92**, 142 (1991).
7. C. R. Evans and J. F. Hawley, Simulation of magnetohydrodynamic flows: A constrained transport method, *Astrophys. J.* **332**, 659 (1988).
8. F. H. Harlow and J. E. Welsch, The MAC method: A computing technique for solving viscous, incompressible, transient fluid flow problems involving free surfaces, *Phys. Fluids* **8**, 2182 (1965).
9. P. Londrillo and L. Del Zanna, High-order upwind schemes for multidimensional magnetohydrodynamics, *Astrophys. J.* **530**, 508 (2000).
10. R. Keppens, G. Tóth, R. H. J. Westermann, and J. P. Goedbloed, Growth and saturation of the Kelvin–Helmholtz instability with parallel and anti-parallel magnetic fields, *J. Plasma Phys.* **61**(1), 1 (1999).

11. K. W. Morton and P. L. Roe, Vorticity-preserving Lax–Wendroff-type schemes for the system wave equation, *SIAM Sci. Comp.* **23**, 170 (2001).
12. K. G. Powell, P. L. Roe, T. J. Linde, T. I. Gombosi, and D. L. De Zeeuw, A solution-adaptive upwind scheme for ideal magnetohydrodynamics, *J. Comput. Phys.* **154**, 284 (1999).
13. D. Ryu, F. Miniati, T. W. Jones, and A. Frank, A divergence-free upwind code for multi-dimensional magnetohydrodynamic flows, *Astrophys. J.* **509**, 244 (1998).
14. I. Sokolov, E. V. Timofeev, J. Sakai, and K. Takayama, On shock-capturing schemes using artificial wind, *Shock Waves J.* **9**, 423 (1999).
15. G. Tóth, The $\nabla \cdot \mathbf{B} = 0$ constraint in shock-capturing magnetohydrodynamics codes, *J. Comput. Phys.* **161**, 605 (2000), doi:10.1006/jcph.2000.6519.
16. K. S. Yee, Numerical solution of initial boundary value problems involving Maxwell's equation in an isotropic media, *IEEE Trans. Antenna Propagation* **AP-14**, 302 (1966).